Desalination and Water Treatment
www.deswater.com

doi: 10.1080/19443994.2015.1052991

57 (2016) 7933–7942
April

Taylor & Francis
Taylor & Francis Group

Isotherm, kinetic, and thermodynamic equations for cefalexin removal from liquids using activated carbon synthesized from loofah sponge

Qiang Kong[a], Yan-na Wang[a], Li Shu[b], Ming-sheng Miao[a,*]

[a] *College of Life Science, Shandong Normal University, 88 Wenhua Donglu, Jinan 250014, Shandong, P.R. China, Tel. +86 531 86180745; emails: kongqiang0531@hotmail.com (Q. Kong), 1461187809@qq.com (Y.-n. Wang), Tel. +86 531 86180745; Fax: +86 531 86180107; email: mingshengmiao@163.com (M.-s. Miao)*

[b] *Faculty of Science, Engineering and Built Environment, School of Engineering, Deakin University, Geelong, Victoria 3216, Australia, email: li.shu846@gmail.com*

Received 17 December 2014; Accepted 12 May 2015

ABSTRACT

Activated carbon (AC) developed from loofah sponge with phosphoric acid activation was applied to absorb cefalexin (CEX) in aqueous solution. AC was characterized by N_2 adsorption–desorption isotherms and Fourier transform infrared spectroscopy (FTIR). Factors influencing the adsorption process were investigated. The equilibrium adsorption isotherms and kinetics of CEX were also studied. The results showed that AC prepared from loofah sponge had rough surface and abundant pores. The determination results of specific surface area (810.12 m^2/g) and average pore size (5.28 nm) suggested the high adsorption capability. At low concentration, the AC could adsorb about 95% of CEX. The adsorption effect was independent of the temperature and pH. The maximum adsorption amount of CEX was about 55.11 mg/g at 308 K. The equilibrium data agreed well with Freundlich isotherm equation ($R^2 = 0.9957$) at 308 K, which indicated multilayer adsorption. FTIR analysis suggested the existence of phosphorus-containing functional groups, C–O bond, and C=C bond on the surface of AC of which the peak intensity of AC after adsorption was slightly lower after adsorption, indicating that the AC surface groups interacted with or were covered by the CEX species.

Keywords: Cefalexin; Adsorption; Activated carbon; Loofah sponge

1. Introduction

Antibiotics are used increasingly in daily life. The addition of antibiotics in animal feed can promote the animal growth. Some antibiotics have a preventive effect against the diseases of livestock and poultry. However, the antibiotics used in large quantities in animal feed are not fully utilized. The antibiotic residue will be discharged into the environment along with the excretions [1]. In some animal food, the antibiotic residue will be transmitted via the food chain. Some of the antibiotics have carcinogenic, teratogenic, and mutagenic effects that interfere with the physiological functions of human body. The metabolites of

---

*Corresponding author.

Presented at the 7th International Conference on Challenges in Environmental Science and Engineering (CESE 2014) 12–16 October 2014, Johor Bahru, Malaysia

antibiotics may not be completely degraded which may result in a major source of antibiotics in water system [2]. These antibiotics pose a great threat to human health [3]. The production of antibiotics will also give rise to wastewater and waste residues containing the antibiotics and the byproducts. Even after treatment, the wastewater still contains antibiotic residues [4]. The sludge produced by wastewater treatment usually adsorbs a large amount of antibiotics [5].

Cefalexin (CEX) is the first-generation cephalosporin antibiotic, with an effective antibacterial effect on Gram-positive bacteria. CEX is usually known for its wide antibacterial spectrum, high efficacy, and less allergic reaction [6]. As more CEX is used in aquaculture, livestock breeding, and agricultural irrigation, a large amount of CEX without being metabolized is directly discharged into the environment. In recent years, the residue of the CEX antibiotic has been detected in a variety of environmental media [7]. The long-term exposure to even trace amounts of CEX antibiotic will cause health problems.

To cope with this potential threat, it is necessary to intensively study the removal of CEX residue [7,8]. However, very few studies have been done in regard to the removal of antibiotics. Ion exchange resin, cellulose, activated carbon (AC), and molecular sieves were used as adsorbents to remove CEX in the water system [9,10]. AC has high specific surface area and abundant pores, which renders excellent adsorption performance. Some studies utilized AC to adsorb the substances that are hard to be degraded in wastewater, typically the heavy metal ions. Dutta et al. [10] discussed the feasibility of using commercialized AC to remove CEX. However, commercialized AC is generally expensive which adds to the total cost of wastewater treatment. Therefore, preparing low-cost and high-efficiency AC is the best choice [11,12].

In this paper, loofah sponge was used as the raw material to prepare the AC which was used to absorb CEX existing in trace amounts from aqueous solutions. Our work may provide a new method for the removal of CEX with loofah sponge.

2. Materials and methods

2.1. Materials and chemicals

Loofah sponge sample was rinsed and the seeds were removed firstly. Then loofah sponge was heated in a muffle furnace at 100℃ for 12 h and processed into the length of about 3–4 mm with a grinder. The minced loofah sponge was dried again at 105℃ for 6 h. Then the sample was placed in a dry beaker, into which appropriate amount of phosphoric acid–deionized water (1:1, v/v) were added (1:5, g/mL) for activation at room temperature for 12 h. The concentration of phosphoric acid was 85%. The loofah sponge sample was carbonized in the resistance box for 2 h at 450℃ [13]. After cooling, the loofah sponge sample was repeatedly rinsed with deionized water until reaching pH value of about 7. The water was discarded, and the sample was dried for 12 h at 120℃ [14]. The loofah sponge sample was taken out after cooling, ground, and screened with 200-mesh sieve. CEX's (CB0280, Life Science Products & Services, China), molecular formula and relative molecular weight were $C_{16}H_{17}N_3O_4S$ and 347.39, respectively; CEX solution used was 100 μmol/L (0.0347 g of CEX was accurately weighed and dissolved in 1,000 mL of deionized water). Other concentrations were obtained by diluting the stock solution with distilled water.

2.2. Characterization of AC

The surface structure of the AC was observed under the scanning electron microscope (SEM). Fourier transform infrared spectroscopy (FTIR) spectrum (400–4,000 cm^{-1}) was analyzed to investigate the influence of adsorption on the functional groups in the AC. In order to reveal the adsorption mechanism, the specific surface area and the average particle size were determined by N_2 static adsorption method. Specific surface area was calculated with BET method to provide reference for the evaluation of adsorption performance of the AC [15].

2.3. Adsorption experiments

The CEX solutions were diluted to different concentration gradients and detected at 268 nm using UV spectrophotometer. The standard curve of concentration vs. absorbance was plotted. After the adsorption experiment, the solution was passed through a 0.22 μ filter membrane and the absorbance was detected. The concentration after adsorption was determined by referring to the standard curve. The equilibrium adsorption amount Q_e and the removal rate η were calculated by formulas (1), (2) and [16], respectively:

$$Q_e = \frac{(C_0 - C_e)V}{W} \tag{1}$$

$$\eta(\%) = \frac{C_0 - C_e}{C_0} \times 100\% \tag{2}$$

where C_0 and C_e are the initial concentration and equilibrium concentration of CEX (mg/L), respectively; V is the volume of solution (L) and W is the mass of AC.

Variable controlling method was employed to discuss the influence of each factor on adsorption. A certain amount of AC was added into the CEX solution with a given initial concentration. After adjusting the desired temperature and pH value, the CEX solution was oscillated and filtrated. The absorbance of the filtrate was determined, and the removal rate and equilibrium adsorption amount of CEX were calculated. Various factors influencing adsorption were investigated in order to find the optimum conditions.

2.4. Adsorption isotherm

Under the temperatures of 288, 298, and 303 K, the adsorption experiment was conducted. CEX was conducted into different concentration solutions (10–100 mg/L), 50 mL was taken out from the 150 mL conical flask, and the addition amount of AC was 1.6 g/L. The sample was oscillated for 4 h in the thermostatic oscillator (180 r/min). After filtration, the absorbance of CEX solution was determined at 268 nm. The equilibrium concentration and equilibrium adsorption amount were calculated. Langmuir, Freundlich, and Dubinin–Radushkevich isotherms were fitted to the experimental data [17,18].

$$Q_e = \frac{Q_m K_L C_e}{1 + K_L C_e} \tag{3}$$

$$\frac{C_e}{Q_e} = \frac{1}{Q_m K_L} + \frac{1}{Q_m} C_e \tag{4}$$

Formula (3) is Langmuir equation and formula (4) is the linear form of formula (3). The equilibrium adsorption amount was predicted using the above formula, which mainly addresses the monolayer adsorption.

Where C_e is the equilibrium adsorption concentration (mg/L); Q_e is equilibrium adsorption amount (mg/g); Q_m is the maximum adsorption capacity (mg/g); and K_L is the Langmuir constant (L/mg), which reflects the adsorption rate. C_e and C_e/Q_e were plotted on the X-axis and Y-axis, respectively. The values of Q_m and K_L were calculated from the slope and intercept of the fitted line.

Freundlich equation can be used to describe multilayer adsorption, with expression (formula (5)) and its linear form (formula (6)) shown below:

$$Q_e = K_F C_e^{\frac{1}{n}} \tag{5}$$

$$\ln Q_e = \ln K_F + \frac{1}{n} \ln C_e \tag{6}$$

where C_e is the equilibrium adsorption concentration (mg/L); Q_e is equilibrium adsorption amount (mg/g); K_F is the Freundlich constant (mg/g); and n is the adsorption intensity, where $1/n$ represents the adsorption capacity, the smaller the $1/n$, the higher the adsorption performance. ln C_e and ln Q_e were plotted on the X-axis and Y-axis, respectively. The values of K_F and $1/n$ were calculated according to the intercept and slope of the fitted line.

Dubinin–Radushkevich equation is shown in formula (7):

$$\ln Q_e = \ln Q_m - \beta \varepsilon^2 \tag{7}$$

$$\varepsilon = RT \ln(1 + 1/C_e) \tag{8}$$

$$E = (2\beta)^{-1/2} \tag{9}$$

where Q_e is the adsorption amount (mg/g) by the adsorbent under adsorption equilibrium; Q_m is the maximum adsorption capacity (mg/g); β is the constant related to the adsorption energy (kJ^2/mol^2); R is the thermodynamic constant; and T is the thermodynamic temperature (K).

C_e is the concentration of the adsorbate under adsorption equilibrium (mol/L); ε is the Polanyi potential; and E is the average free energy of adsorption (kJ/mol). ε^2 and ln Q_e were plotted on the X-axis and Y-axis, respectively. The values of Q_m and β could be known from the intercept and slope of the fitted line, and hence the E value was obtained.

2.5. Adsorption kinetics

Adsorption kinetics data were analyzed by the three most widely used kinetic models, the pseudo-first-order, the pseudo-second-order models, and the intraparticle diffusion model.

The linear form of the pseudo-first-order equation (10) can be expressed as

$$\ln(Q_e - Q_t) = \ln Q_e - k_1 t \tag{10}$$

where Q_e and Q_t (mg/g) are the amounts of CEX adsorbed at equilibrium and at time t (min), respectively, and k_1 (1/min) is the rate constant of the pseudo-first-order model. The values of Q_e and k_1 can be obtained from the intercept and slope of a plot of ln(Q_e − Q_t) vs. t.

The linear form of the pseudo-second-order model equation [19] is given as follows:

$$t/Q_t = 1/k_2 Q_e^2 + t/Q_e \tag{11}$$

where Q_e is the amount of Cr(VI) adsorbed at equilibrium (mg/g), Q_t is the amount of Cr(VI) adsorbed at time t (mg/g), k_2 is the rate constant of the pseudo-second-order model (g/(mg min)) and t is the time (min). The parameters Q_e and k_2 can be estimated from the slope and intercept of a plot of (t/Q_t) vs. t, respectively.

To identify the diffusion mechanism in the CEX/AC system, the intraparticle diffusion model is considered using the following [20]:

$$Q_t = k_p t^{1/2} + C \tag{12}$$

where k_p is the intraparticle diffusion rate constant (mg/(g min$^{1/2}$)) and C is the intercept (mg/g). k_p and C can be obtained from a plot (Q_t) vs. $t^{1/2}$. Intraparticle diffusion is the sole rate-limiting step if the plot of (Q_t) vs. $t^{1/2}$ is a straight line that passes through the origin [21].

2.6. Thermodynamics

In order to gain a better understanding of the adsorption mechanism, the free energy changes (ΔG), enthalpy change (ΔH), and entropy change (ΔS) were studied.

Eq. (13) was used to compute the Gibbs free energy of adsorption [22], and the standard enthalpy change and entropy change of the CEX reduction are related to the Langmuir coefficient by Eq. (14).

$$\Delta G = -RT \ln K_L \tag{13}$$

$$\ln K_L = \Delta S/R - \Delta H/RT \tag{14}$$

where R is the ideal gas constant (8.314 J/(mol K)), T is the thermodynamic temperature (K), and K_L is the Langmuir coefficient (L/mol).

3. Results and discussion

3.1. Characteristics of AC

The surface structure of the AC determines the adsorption performance to a certain extent [23]. Fig. 1(a) is the SEM image of AC prepared from loofah sponge and Fig. 1(b) is the SEM image of the raw loofah sponge. It can be seen from (a) that the AC surface was irregular with non-uniform pore size distribution. Porosity and roughness are two basic features of the surface of AC. Fig. 1(b) showed that the surface of the raw loofah sponge was polyporous. SEM images show the fibrous structure of AC, which may be due to inherent fiber structure in the raw loofah sponge [24].

According to the surface area analyzer, the specific surface area of the AC was 810.12 m^2/g and the average pore size was 5.28 nm. The results (Fig. 2) indicated that the AC had developed pores inside, which were mainly micropores and mesopores . Thus, the AC prepared from loofah sponge may have excellent adsorption performance.

3.2. Effect of contact time

Firstly, 50 mL of CEX solution (100 μmol/L) was taken out from the 150 mL conical flask, and the addition amount of AC was 1.0 g/L. The sample was oscillated for 360 min in the thermostatic oscillator (180 r/min), every once in a while sampling when oscillating, and the sampling times were 10, 30, 60, 90, 120, 180, 240, 300, and 360 min. After filtration, the absorbance of CEX solution was determined at 268 nm. The equilibrium concentration and equilibrium adsorption amount were calculated. It can be seen from Fig. 3 that the removal rate rose steadily within the first 90 min, initially from 71.58 to 82.04%. After 90 min, the increase in removal rate was slowed down. The peak of 85.3% occurred at 240 min, beyond which no further changes took place. The variation trend of adsorption amount was similar to that of the removal rate, that is, there was a sharp increase at the beginning, followed by a slower increase. The final adsorption amount was about 28.93 mg/g. Based on this result, 180 min was finally determined as the time when adsorption equilibrium was reached.

3.3. Effect of temperature

Temperature is one of the important parameters to study in adsorption experiments [25]. Fifty milliliters of CEX solution (100 μmol/L) was taken out from the 150 mL conical flask, and the addition amount of AC was 1.6 g/L. Under the temperature of 288, 298, and 308 K, the sample was oscillated for 4 h in the thermostatic oscillator (180 r/min). After filtration, the absorbance of CEX solution was determined at 268 nm. The equilibrium concentration and equilibrium adsorption amount were calculated. It can be seen from Fig. 4 that temperature had a very small influence on the adsorption, with no distinct variation trend. In the adsorption experiment, the removal rate fluctuated in the range of 93.8–95.08%, higher than Trapa natans husk-based AC (89.4%) [1]. With increasing temperature, the adsorption capacity did not change and

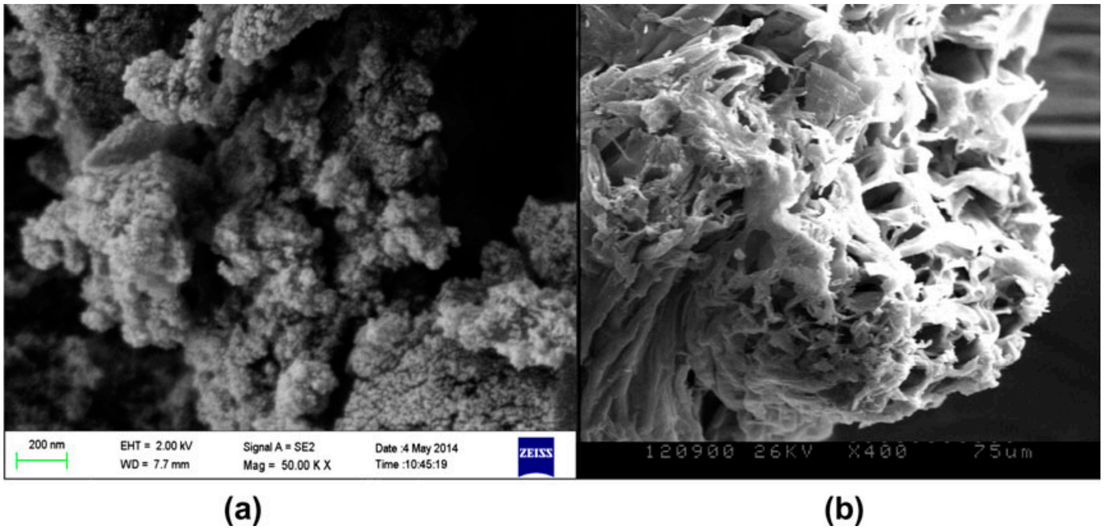

Fig. 1. SEM image of AC developed from loofah sponge (a) and SEM images for raw loofah sponge (b).

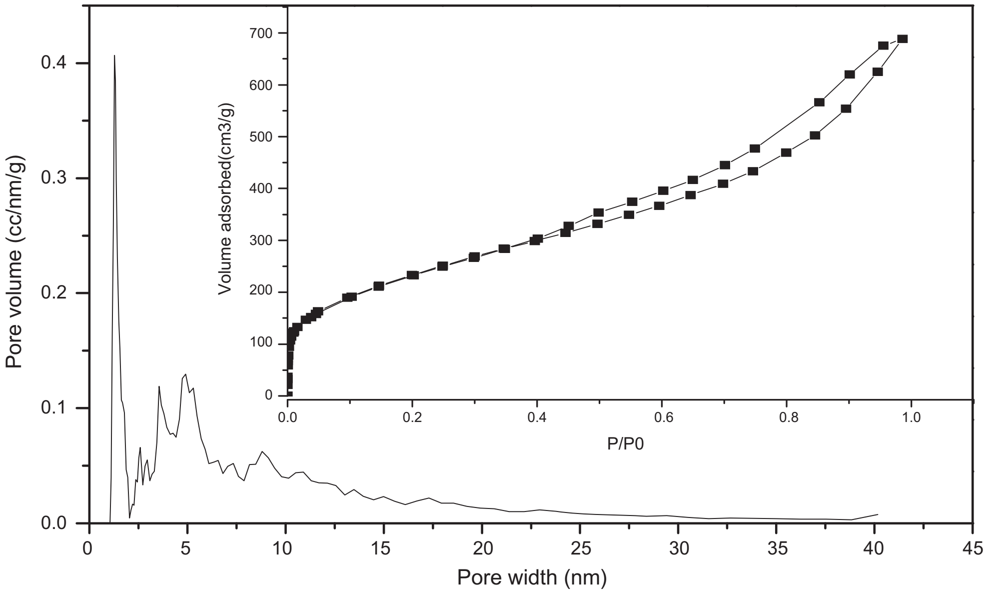

Fig. 2. Pore size distribution of AC prepared from loofah sponge (the figure shows the $\mathbf{N_2}$ adsorption–desorption isotherm of AC).

remained around 20.7 mg/g, which showed that the effect of temperature on adsorption was negligible. In the present experiment, the influence of temperature on the adsorption effect was negligible.

3.4. Effect of AC content

The addition amount of AC significantly influences the adsorption effect and the adsorption. Fifty milliliters of CEX solution (100 μmol/L) was taken out from the 150 mL conical flask, and the addition amount of AC was 0.2–2.0 g/L. The sample was oscillated for 4 h in the thermostatic oscillator (180 r/min). After filtration, the absorbance of CEX solution was determined at 268 nm. The equilibrium concentration and equilibrium adsorption amount were calculated. Fig. 5 showed the influence of the amount of AC added on removal rate and equilibrium adsorption amount. As the amount of AC increased, the removal rate of CEX increased. The increase rate was high at the beginning

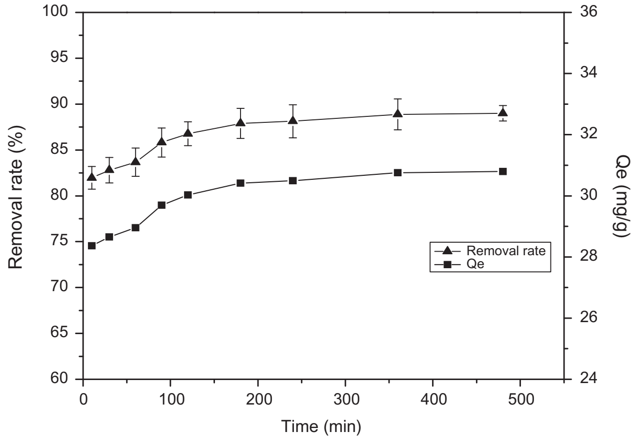

Fig. 3. Effect of contact time on removal rate and adsorption amount (AC content = 1 g/L; the initial concentration = 100 μmol/L; and temperature = 25℃).

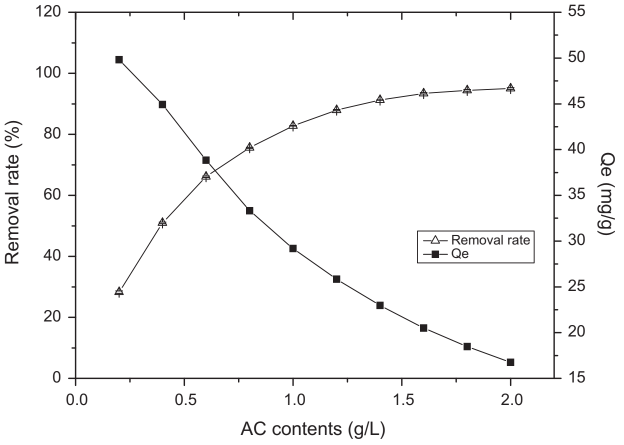

Fig. 5. Influence of AC content on removal rate and adsorption capacity (temperature = 30℃; the initial concentration = 100 μmol/L; and time = 4 h).

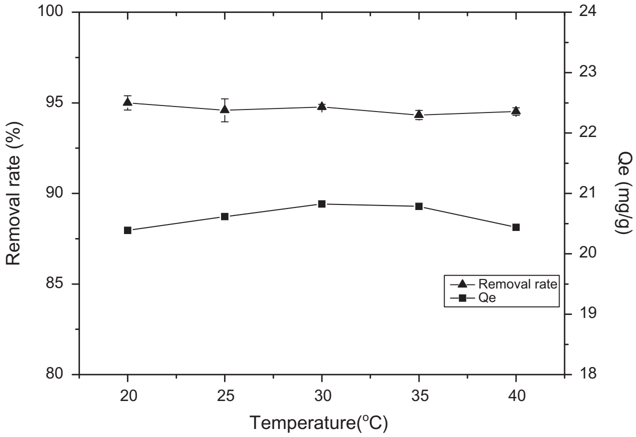

Fig. 4. Influence of temperature on removal rate and adsorption amount (AC content = 1.6 g/L; the initial concentration = 100 μmol/L; and time = 4 h).

and gradually became stable. At the addition amount of 1.6 g/L, the removal rate reached stability, the value being 93%.

In contrast to the trend of removal rate, the equilibrium adsorption amount decreased with the increase in the amount of AC addition. The reason may be that in the presence of abundant adsorbent, there was the phenomenon of competitive adsorption [26]. As the addition amount of AC continued to increase, almost all the CEX in the solution was adsorbed without reaching the state of saturation adsorption. When the addition amount of AC was 0.2 g/L, the maximum adsorption amount was 49.82 mg/g.

3.5. Effect of initial solution pH

Fifty milliliters of CEX solution (100 μmol/L) was taken out from the 150 mL conical flask, the initial solution pH was adjusted to 1–14 with phosphoric acid or NaOH solution, and the addition amount of AC was 1.6 g/L. The sample was oscillated for 4 h in the thermostatic oscillator (180 r/min). After filtration, the absorbance of CEX solution was determined at 268 nm. The equilibrium concentration and equilibrium adsorption amount were calculated. It can be seen from Fig. 6 that pH value had a negligible effect on adsorption under acidic and neutral conditions. The inhibitory effect was great on the removal rate and equilibrium adsorption amount only under strongly alkaline condition. When pH value was smaller than 11, the removal rate and the equilibrium adsorption amount remained basically stable. The removal rate was 92.46–94.09%, and the equilibrium adsorption amount was 20.23–20.59 mg/g. When the pH value increased to a certain level, the removal rate and the equilibrium adsorption amount decreased to 69.1% and 15.16 mg/g, respectively. The reason is that at high pH, the weakly acidic functional groups on the surface of AC would be deprotonated. Then, the net negative charges increase with the increase in pH [1]. Hence, the electrostatic repulsion would increase inaction CEX ions with the surface of AC.

3.6. Effect of initial concentration

In order to discuss the influence of initial concentration of CEX on adsorption, gradient concentration of CEX solutions (10–100 mg/L) were prepared, 50 mL

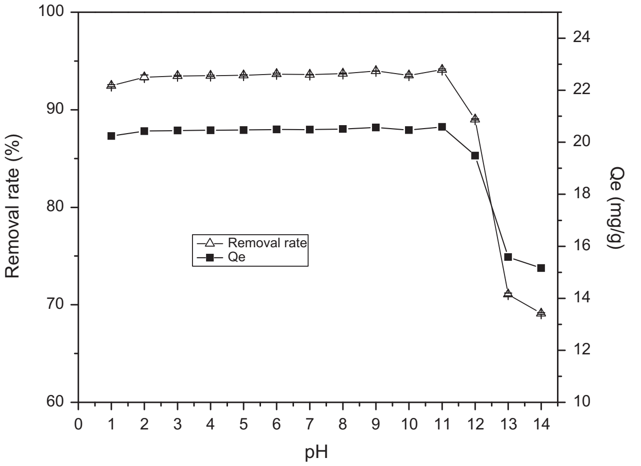

Fig. 6. Influence of solution pH on removal rate and adsorption capacity (AC content = 1.6 g/L; temperature = 30℃; the initial concentration = 100 μmol/L; and time = 4 h).

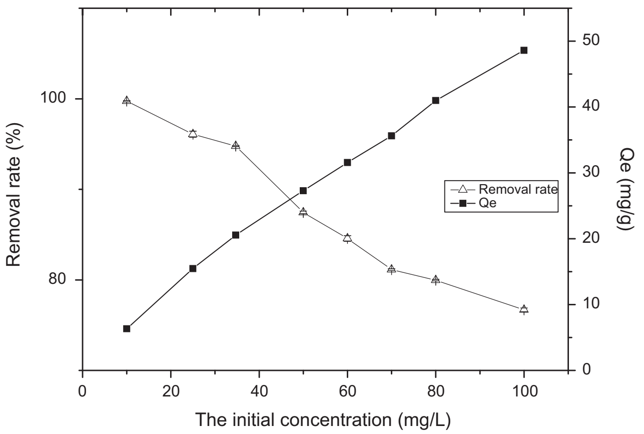

Fig. 7. Effect of the initial concentration on the adsorption capacity of AC and removal rate (AC content = 1.6 g/L; temperature = 30℃; and time = 4 h).

was taken out from the 150 mL conical flask, and the addition amount of AC was 1.6 g/L. The sample was oscillated for 4 h in the thermostatic oscillator (180 r/min). After filtration, the absorbance of CEX solution was determined at 268 nm. The absorbance was detected after the adsorption process. The removal rates and equilibrium adsorption amounts were calculated.

As shown in Fig. 7, initial concentration had a huge influence on removal rate and adsorption amount. As the initial concentration increased, the removal rate decreased, roughly in a linear trend. On the contrary, the adsorption amount increased steadily, with the maximum reaching 48.61 mg/g. This value was comparable with 49.82 mg/g, which was the maximum adsorption amount when the addition amount of AC was 0.2 g/L. This indicated that the maximum adsorption amount of CEX from aqueous solutions by AC was about 55.11 mg/g.

3.7. FTIR analysis

Infrared spectroscopy is a technical tool that is increasingly applied to discuss the adsorption mechanism. The characteristics of functional groups on the surface of AC were visualized by the analysis of adsorption spectra (Fig. 8).

FTIR analysis suggested the existence of phosphorus-containing functional groups, C–O bond, and C=C bond on the surface of AC of which the peak intensity of AC after adsorption was slightly lower after adsorption, indicating that the AC surface groups interacted with or were covered by the CEX species. The absorption peak at 1,570–1,700 cm^{-1} was weakened, probably due to the reduction of C=O bond. The peaks at 1,600 cm^{-1} corresponded to the benzene ring or C=C bond, respectively, which were caused by stretching vibration. The reason was the formation of functional groups containing carbonyl and the aromatic compounds containing benzene ring during the preparation process [27]. The absorption peak at 900–1,300 cm^{-1} was attributed to the phosphorus-containing functional group. After phosphoric acid activation, phosphorus-containing functional group was produced on the surface of the AC [28]. It was believed that the absorption peak at 1,100 cm^{-1} was due to the stretching vibration of C–O bond. It is generally considered that the absorption peak at 400–1,000 cm^{-1} is caused by

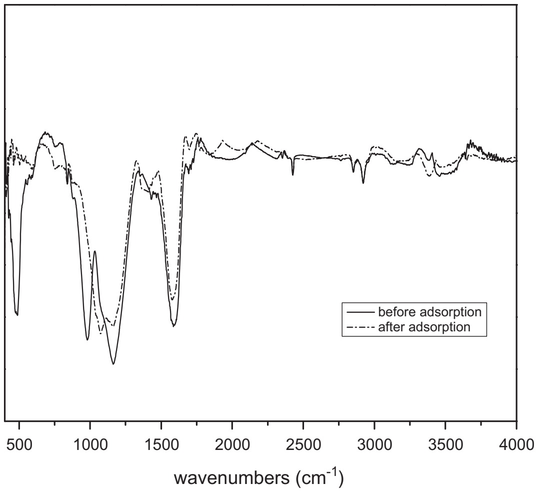

Fig. 8. FTIR spectra of AC before and after adsorption.

Table 1
The relevant parameters of the three adsorption isotherms

		Langmuir			Freundlich			Dubinin–Radushkevich			
Adsorption temperature (K)	Q_{exp} (mg/g)	Q_{m} (mg/g)	K_{L} (L/mg)	R^2	$1/n$	K_{F} $(\mathrm{mg/g})^{1/n}$	R^2	Q_{m} (mg/g)	E (kJ/mol)	β ($\mathrm{kJ^2/mol^2}$)	R^2
288	50.856	51.282	0.251	0.9260	0.350	14.588	0.9948	157.938	14.142	0.0025	0.9889
298	48.616	49.261	0.338	0.9419	0.294	17.138	0.9862	114.217	16.667	0.0018	0.9679
308	55.105	58.824	0.565	0.9706	0.423	19.603	0.9957	297.615	14.142	0.0025	0.9979

Table 2
Kinetic parameters of CEX on AC

		The pseudo-first-order model			The pseudo-second-order model				The intraparticle diffusion model		
Adsorption temperature (K)	Q_{exp} (mg/g)	k_1 ($\mathrm{min^{-1}}$)	Q_{e} (mg/g)	R^2	k_2 (g/(mg min))	Q_{e} (mg/g)	V_0 (mg/(g min))	R^2	k_{p} $(\mathrm{mg/(g\ min)^{1/2}})$	C (mg/g)	R^2
288	29.797	0.014	100.796	0.7204	0.005	29.674	4.464	0.9989	0.328	23.604	0.9044
298	30.797	0.008	8.972	0.8811	0.011	30.960	10.215	0.9990	0.168	27.893	0.9462
308	33.273	0.010	12.920	0.6976	0.011	33.333	12.005	0.9999	0.203	29.785	0.8576

Table 3
Thermodynamic parameters of CEX on AC

Temperature (K)	K (L/mol)	ΔG (kJ/mol)	ΔS (J/(mol K))	ΔH (kJ/mol)
288	87.195	−1.070	140.357	2.982
298	117.818	−1.181		
308	196.275	−1.352		

M–O bond and M–OH bond (M represents a metal element) [29]. Therefore, before the adsorption experiment, the absorption peak at 489.37 $\mathrm{cm^{-1}}$ could be attributed to M–O bond or M–OH bond, which was destroyed because of adsorption.

3.8. Adsorption isotherms

Adsorption isotherms are critical to evaluate the sorption capacity of adsorbents as well as to understand the nature of sorbate–sorbent interactions. After data fitting, the fitting degree R^2 was 0.9260, 0.9948, and 0.9889 for the Langmuir, Freundlich, and Dubinin–Radushkevich equations at 288 K, respectively. The parameters of adsorption isotherm models for CEX were depicted in Table 1. Based on the data in Table 1, the equilibrium data agreed well with the Freundlich isotherm equation. This result indicated the occurrence of multilayer adsorption [30]. The relevant parameter of the Freundlich constant $1/n$ was less than 1, indicating a favorable adsorption process [30].

3.9. Adsorption kinetics and thermodynamics

3.9.1. Adsorption kinetics

All of the kinetic parameters and correlation coefficients for the CEX/AC system were listed in Table 2. Compared with the pseudo-first-order model and the rate of intraparticle diffusion, the pseudo-second-order model fitted the experimental data quite well and R^2 analyses supported this conclusion. There was good agreement between Q_{e} and Q_{exp}. R^2 were 0.9989, 0.9990, and 0.9999 for the pseudo-second-order model at 288, 298, and 308 K, respectively. With the increase in the temperature, the fit of the pseudo-second-order model was better. C indicates the boundary thickness, so the larger the C is, the greater the effect of the boundary. The *C* of the intraparticle diffusion rate was bigger for 308 K than 288 K; it meant that with lower temperature, the effect of the boundary decreased.

Overall, the results suggested that the adsorption of CEX by AC might be a pseudo-second-order reaction, based on the assumption that between sorbent and sorbate, the rate-limiting step might be chemisorption (including valence forces through the sharing or exchange of electrons) or chemical sorption [31].

3.9.2. Thermodynamics

As Table 3 showed, ΔG, ΔH, and ΔS were −1.07 kJ/mol, 140.357 J/(mol K), and 2.982 kJ/mol at 288 K, respectively. ΔG was negative at all temperatures, which meant that the adsorption process was spontaneous in nature. The positive value of ΔH indicated the endothermic nature of the process of adsorption. The positive value of ΔS confirmed that there was an increase in randomness at the solid/solution interface occurring at the internal structure of the adsorption of CEX on AC [32].

4. Conclusion

The AC prepared from loofah sponge with phosphoric acid activation has a large specific surface area and contains large amounts of micropores and mesopores. Therefore, it can serve as a high-performance adsorbent. Under low concentration, the AC could adsorb about 95% of CEX. The AC prepared from loofah sponge did not have a high requirement on the adsorption conditions. The reaction conditions were mild and could be easily achieved. The maximum adsorption amount of CEX was about 55.11 mg/g. FTIR analysis showed that the surface of AC prepared from loofah sponge was abundant in phosphorus-containing functional groups, C–O bond, and C=C bond of which the peak intensity of AC after adsorption decreased, indicating that the AC surface groups interacted with or were covered by the CEX species. The equilibrium data agreed well with the Freundlich isotherm equation, which indicated multilayer adsorption, and the adsorption of CEX by AC might be a pseudo-second-order reaction. Thermodynamics indicated the endothermic and spontaneous natures of the adsorption process.

Acknowledgments

This work was supported by the Promotive research fund for excellent young and middle-aged scientists of Shandong Province (No. BS2014HZ019), A Project of Shandong Province Higher Educational Science and Technology Program (No. J15LE07), the Project funded by China Postdoctoral Science Foundation (No. 2014M551950), and the Major Science and Technology Program for Water Pollution Control and Treatment (2012ZX07203004 and 2015ZX07203005).

References

[1] W. Liu, H. Xie, J. Zhang, C. Zhang, Sorption removal of cephalexin by HNO_3 and H_2O_2 oxidized activated carbons, Sci. China Chem. 55 (2012) 1959–1967.

[2] P.A. Blackwell, P. Kay, R. Ashauer, A.B.A. Boxall, Effects of agricultural conditions on the leaching behaviour of veterinary antibiotics in soils, Chemosphere 75 (2009) 13–19.

[3] P.A. Blackwell, P. Kay, A.B.A. Boxall, The dissipation and transport of veterinary antibiotics in a sandy loam soil, Chemosphere 67 (2007) 292–299.

[4] W. Liu, J. Zhang, C. Zhang, L. Ren, Sorption of norfloxacin by lotus stalk-based activated carbon and iron-doped activated alumina: Mechanisms, isotherms and kinetics, Chem. Eng. J. 171 (2011) 431–438.

[5] V. Chitnis, S. Chitnis, K. Vaidya, S. Ravikant, S. Patil, D.S. Chitnis, Bacterial population changes in hospital effluent treatment plant in central India, Water Res. 38 (2004) 441–447.

[6] A. Ledezma Estrada, Y.-Y. Li, A. Wang, Biodegradability enhancement of wastewater containing cefalexin by means of the electro-fenton oxidation process, J. Hazard. Mater. 227–228 (2012) 41–48.

[7] B. Lin, J. Lyu, X.-J. Lyu, H.-Q. Yu, Z. Hu, J.C.W. Lam, P.K.S. Lam, Characterization of cefalexin degradation capabilities of two Pseudomonas strains isolated from activated sludge, J. Hazard. Mater. 282 (2015) 158–164.

[8] X. Lu, G. Zhen, Y. Liu, T. Hojo, A.L. Estrada, Y.-Y. Li, Long-term effect of the antibiotic cefalexin on methane production during waste activated sludge anaerobic digestion, Bioresour. Technol. 169 (2014) 644–651.

[9] M. Grassi, L. Rizzo, A. Farina, Endocrine disruptors compounds, pharmaceuticals and personal care products in urban wastewater: Implications for agricultural reuse and their removal by adsorption process, Environ. Sci. Pollut. Res. 20 (2013) 3616–3628.

[10] M. Dutta, N.N. Dutta, K.G. Bhattacharya, Aqueous phase adsorption of certain beta-lactam antibiotics onto polymeric resins and activated carbon, Sep. Purif. Technol. 16 (1999) 213–224.

[11] J.L. Martinez, Environmental pollution by antibiotics and by antibiotic resistance determinants, Environ. Pollut. 157 (2009) 2893–2902.

[12] J. Rivera-Utrilla, M. Sánchez-Polo, M.Á. Ferro-García, G. Prados-Joya, R. Ocampo-Pérez, Pharmaceuticals as emerging contaminants and their removal from water, Chemosphere 93 (2013) 1268–1287.

[13] H. Liu, P. Dai, J. Zhang, C. Zhang, N. Bao, C. Cheng, L. Ren, Preparation and evaluation of activated carbons from lotus stalk with trimethyl phosphate and tributyl phosphate activation for lead removal, Chem. Eng. J. 228 (2013) 425–434.

[14] H. Liu, Q. Gao, P. Dai, J. Zhang, C. Zhang, N. Bao, Preparation and characterization of activated carbon from lotus stalk with guanidine phosphate activation: Sorption of Cd(II), J. Anal. Appl. Pyrol. 102 (2013) 7–15.

[15] H. Liu, J. Zhang, N. Bao, C. Cheng, L. Ren, C. Zhang, Textural properties and surface chemistry of lotus stalk-derived activated carbons prepared using different phosphorus oxyacids: Adsorption of trimethoprim, J. Hazard. Mater. 235–236 (2012) 367–375.

[16] H. Liu, J. Zhang, W. Liu, N. Bao, C. Cheng, C. Zhang, Preparation and characterization of activated charcoals from a new source: Feather, Mater. Lett. 87 (2012) 17–19.

[17] Q. Gao, H. Liu, C. Cheng, K. Li, J. Zhang, C. Zhang, Y. Li, Preparation and characterization of activated carbon from wool waste and the comparison of muffle furnace and microwave heating methods, Powder Technol. 249 (2013) 234–240.

[18] H. Liu, W. Liu, J. Zhang, C. Zhang, L. Ren, Y. Li, Removal of cephalexin from aqueous solutions by original and Cu(II)/Fe(III) impregnated activated carbons developed from lotus stalks kinetics and equilibrium studies, J. Hazard. Mater. 185 (2011) 1528–1535.

[19] P. Yuan, M. Fan, D. Yang, H. He, D. Liu, A. Yuan, J. Zhu, T. Chen, Montmorillonite-supported magnetite nanoparticles for the removal of hexavalent chromium from aqueous solutions, J. Hazard. Mater. 166 (2009) 821–829.

[20] W.J. Weber, J.C. Morris, Kinetics of adsorption on carbon from solution, J. Sanit. Eng. Div. Am. Soc. Civ. Eng. 89 (1963) 31–59.

[21] Ö. Gerc, A. Özcan, A.S. Özcan, H.F. Gerc, Preparation of activated carbon from a renewable bio-plant of Euphorbia rigida by H_2SO_4 activation and its adsorption behavior in aqueous solutions, Appl. Surf. Sci. 253 (2007) 4843–4852.

[22] S.H. Chen, Q.Y. Yue, B.Y. Gao, Q. Li, X. Xu, Removal of Cr(VI) from aqueous solution using modified corn stalks: Characteristic, equilibrium, kinetic and thermodynamic study, Chem. Eng. J. 168 (2011) 909–917.

[23] J. Fan, J. Zhang, C. Zhang, L. Ren, Q. Shi, Adsorption of 2,4,6-trichlorophenol from aqueous solution onto activated carbon derived from loosestrife, Desalination 267 (2011) 139–146.

[24] O. Abdelwahab, Evaluation of the use of loofah activated carbons as potential adsorbents for aqueous solutions containing dye, Desalination 222 (2008) 357–367.

[25] L. Ren, J. Zhang, Y. Li, C. Zhang, Preparation and evaluation of cattail fiber-based activated carbon for 2,4-dichlorophenol and 2,4,6-trichlorophenol removal, Chem. Eng. J. 168 (2011) 553–561.

[26] M. Miao, Y.Wang, Q. Kong, L. Shu, Adsorption kinetics and optimum conditions for Cr(VI) removal by activated carbon prepared from luffa sponge, Desalin. Water Treat. (2015) 1–10, doi: 10.1080/19443994.2015.1015453.

[27] Y. Guo, D.A. Rockstraw, Activated carbons prepared from rice hull by one-step phosphoric acid activation, Micropor. Mesopor. Mat. 100 (2007) 12–19.

[28] A.M. Puziy, O.I. Poddubnaya, Synthetic carbons activated with phosphoric acid: I. Surface chemistry and ion binding properties, Carbon 40 (2002) 1493–1505.

[29] Z. Ai, Y. Cheng, L. Zhang, J. Qiu, Efficient to removal of Cr(VI) from aqueous solution with $Fe@Fe_2O_3$ core-shell nanowires, Environ. Sci. Technol. 42 (2008) 6955–6960.

[30] W. Liu, J. Zhang, C. Cheng, G. Tian, C. Zhang, Ultrasonic-assisted sodium hypochlorite oxidation of activated carbons for enhanced removal of Co(II) from aqueous solutions, Chem. Eng. J. 175 (2011) 24–32.

[31] Y.S. Ho, G. McKay, Pseudo-second order model for sorption processes, Process Biochem. 34(5) (1999) 451–465.

[32] S. Yadav, V. Srivastava, S. Banerjee, C.H. Weng, Y.C. Sharma, Adsorption characteristics of modified sand for the removal of hexavalent chromium ions from aqueous solutions: Kinetic, thermodynamic and equilibrium studies, Catena 100 (2012) 120–127.